JACS
JOURNAL OF THE AMERICAN CHEMICAL SOCIETY

Article

pubs.acs.org/JACS

Probing Electric Field Effect on Covalent Interactions at a Molecule–Semiconductor Interface

Papatya C. Sevinc, Bharat Dhital, Vishal Govind Rao,[†] Yuanmin Wang,[†] and H. Peter Lu*

Department of Chemistry and Center for Photochemical Sciences, Bowling Green State University, Bowling Green, Ohio 43403, United States

Supporting Information

ABSTRACT: Fundamental understanding of the energetic coupling properties of a molecule–semiconductor interface is of great importance. The changes in molecular conformations and vibrational modes can have significant impact on the interfacial charge transfer reactions. Here, we have probed the change in the interface properties of alizarin–TiO_2 system as a result of the externally applied electric field using single-hot spot microscopic surface-enhanced Raman spectroscopy (SMSERS) and provided a theoretical understanding of our experimental results by density functional theory (DFT) calculations. The perturbation, caused by the external potential, has been observed as a shift and splitting of the 648 cm^{-1} peak, typical indicator of the strong coupling between alizarin and TiO_2, at SMSERS. On the basis of our experimental results and DFT calculations, we suggest that electric field has significant effects on vibrational coupling at the molecule–TiO_2 interface. The presence of perturbed alizarin–TiO_2 coupling under interfacial electric potential may lead to changes in the interfacial electron transfer dynamics. Additionally, heterogeneously distributed dye molecules at the interface on nanometer length scale and different chromophore-semiconductor binding interactions under charge accumulation associated interfacial electric field changes create intrinsically inhomogeneous interfacial ET dynamics associated with both static and dynamic disorders.

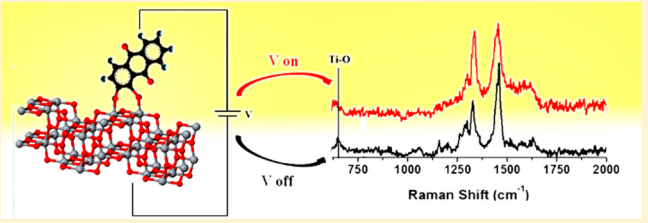

1. INTRODUCTION

Interfacial electron transfer (ET) at molecule–semiconductor interfaces has been intensively investigated due to its crucial role in fundamental chemistry and physics, as well as in extensive applications like solar energy conversion, molecular devices, and photocatalysis.[1−3] In those systems, titanium dioxide (TiO_2) has been the most widely used and investigated semiconductor material due to its molecule–surface chemical interactions, large band gap, photostability, nontoxicity, and low cost. It has been reported that the dynamics of interfacial ET is directly related to the properties of the molecule–TiO_2 interface such as the electronic coupling, the vibrational relaxation energy of the adsorbed molecules and the local solvent, surface vibrational modes of the semiconductor.[1−4] Furthermore, electrical potential difference created either by the system or applied externally to drive the system is known to perturb the vibrational energy levels of the adsorbed molecules on the TiO_2 surface,[5,6] which is typically reflected in the vibrational spectra as a linear frequency shift.[7,8] However, even though it is known that electrostatic fields can extensively affect the physical properties of molecules[9] including the interface properties[10] as well as the ET dynamics, the consequences of the electric potential applied to the system and/or created by the system to the molecule–semiconductor interface still requires a fundamental understanding. In this article, we investigate electric field effect (EFE) at the alizarin–TiO_2 interface by using single-hot spot microscopic surface-enhanced Raman spectroscopy (SMSERS). Our technique also utilizes the charge transfer enhanced Raman scattering mechanism by laser excitation at the charge transfer absorption band at 488 nm,[11] which gives the vibrational fingerprint information on the molecule–TiO_2 interactions critical for the spectral and energetic characterization of the interfacial electron transfer dynamics.[12−17]

EFE has been analyzed theoretically and reported extensively over the last 40 years;[7,18−27] although, quantitative experimental results have only been introduced in the last two decades.[8,28−39] Early studies of the EFE have focused only on changes in molecular geometry, considering that for a static geometry, within the harmonic approximation, there will be no dipole moment dependence of the vibrational levels.[18] Later, it has been recognized that anharmonicity constitutes the origin of EFE.[21] Anharmonic contributions have been separated into two parts:[27] (i) mechanical anharmonicity, in which the interaction with the electric field causes the dipole moment to change due to the anharmonicity of the potential energy surface; and (ii) electrical anharmonicity, which causes perturbation of the harmonic bond force constant resulting in change in the transition energy between the vibrational levels.[26,30,31,36,40−42] Furthermore, the relationship between the bond length and the force constant is described by Badger's

Received: September 30, 2015
Published: January 6, 2016

DOI: 10.1021/jacs.5b10253
J. Am. Chem. Soc. 2016, 138, 1536−1542

rule which suggests that the changes in molecular geometry would result in vibrational frequency shifts.[43] The amount of shift observed is directly related to the strength of the electric field and its interaction with the molecule, according to reports of the detailed theoretical studies.[8,12,24,30,31,40−42,44−46] Previously, EFE has been predominantly applied to investigate the electric fields in protein cavities and how they change as a result of interactions with ligand or another protein by using the sensitivity of some specific groups like nitriles, and carbon monoxides.[32,36,38−42,46,47] Moreover, EFE has been used to study the diffuse double-layer structure at electrochemical interfaces to get an insight into electrochemical processes dependent on interfacial ET.[34,35,48−50]

In this paper, we have chosen alizarin−TiO_2 system because of its strong electronic coupling at the interface which has been demonstrated by the previous infrared data and structure analysis calculations.[51−56] The alizarin−TiO_2 system is particularly interesting because interfacial ET is essentially ultrafast in femtosecond range, whereas alizarin excited state is at the edge of the conduction band (CB) of TiO_2, where the TiO_2 density of state (DOS) is lowest.[3] Interfacial ET is sensitive to the energetics of both dye molecules and the semiconductors, the DOS, the magnitude and energy dependence of the dye−semiconductor electronic and vibrational coupling, and the vibrational relaxation dynamics.[3] Earlier studies suggest that when the DOS and the dye−semiconductor coupling change slowly over the relevant energy range, interfacial ET is well described by the pure electronic limit without vibrational contributions. However, when the DOS and the dye−semiconductor coupling vary significantly over the relevant energy range, the interfacial ET depends substantially on the vibrational Franck−Condon factors.[3] For alizarin−TiO_2 system, the electronic coupling between alizarin and the semiconductor vary significantly even within a small energy range, which makes the alizarin−TiO_2 system highly susceptible toward an applied electric field.[3] Our results as well as the literature reports suggest that the covalent bonding of the alizarin molecule to Ti atoms through hydroxyl groups gives rise to an additional peak at 648 cm^{-1} in the Raman spectra.[11a,53,57,58] The strong electronic coupling makes this molecule−semiconductor system valuable to study the effects of applied electric field at the interface by using our SMSERS imaging analysis. Fundamental understanding of this phenomenon is critically related to the manipulation and design of many applications like photovoltaic devices and molecular electronics.

2. EXPERIMENTAL SECTION

Materials and Sample Preparation. Alizarin, $AgNO_3$, NH_2OH·HCl, and NaOH were purchased from Sigma-Aldrich and used as received. Silver nanoparticles (Ag NPs) were synthesized by reduction of $AgNO_3$ by NH_2OH·HCl as described elsewhere.[59] The average size of the Ag NP is ∼50 nm as identified by TEM. Additionally, to activate the Ag NP for SERS measurements, NaCl is added to the Ag NP solution. TiO_2 NP (size ∼13 nm as determined by AFM) was prepared by using $Ti(OCH-(CH_3)_2)_4$ (Sigma-Aldrich) as precursor according to the literature.[60] Aeroxide TiO_2 P25 and ITO coverslips (18 mm × 18 mm, 8−12 ohms) were purchased from Nippon Aerosil Co. Ltd. and SPI supplies, respectively. ITO coverslips were thoroughly cleaned by sonication in deionized water, acetone, isopropyl alcohol and deionized water, each for 15 min, and dried in a jet of nitrogen gas before their use. All solvents used were of HPLC grade.

The aqueous solution of 0.1 mM TiO_2 P25 was air-dried and then annealed at 400 °C for 1 h on cleaned ITO surface (∼70 nm thickness). Then 5×10^{-8} M Alizarin incubated with TiO_2 NP and Ag NP was air-dried on TiO_2 layer. Finally to connect the electrode, a silver layer was sputter coated (Cressington Sputter Coater) on the sample surface for 60 s (∼50 nm in thickness). The electrodes are connected to silver layer and ITO coverslip to apply potential (Figure 1A).

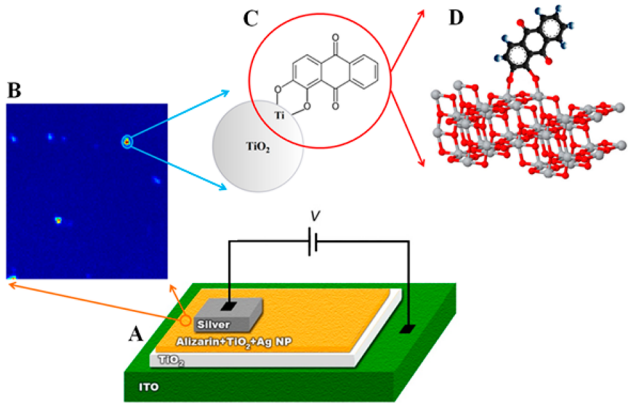

Figure 1. (A) Schematic representation of the experimental setup. (B) Optical imaging of the sample surface (20 μm × 20 μm). (C) Schematic representation of the alizarin−TiO_2 system. (D) Alizarin binding to TiO_2 surface (red, oxygen; gray, titanium; dark gray, carbon; and blue, hydrogen). During our potential measurements, it has been assumed that all layers experience the applied potential without any losses from layer to layer.

Surface-Enhanced Raman and Potential Measurements. SMSERS imaging (Figure 1B) is recorded by an Axiovert 135 inverted scanning confocal microscope, equipped with a 100 × 1.3 NA oil immersion objective (Zeiss FLUAR). A continuous-wave (CW) laser (488 nm, Melles-Griot) is used to pump the sample at 10 μW for SERS measurements. A beam splitter ZT488rdc (Chroma) is used to reflect the excitation light into the microscope objective. Before the scattered light focusing into a monochromator (Triax 550, Jobin Yvon), a band-pass filter HHQ495LP is positioned before the entrance slit to further eliminate the Rayleigh light. The Raman spectra are collected by a LN-CCD (Princeton Instruments) cooled at about −100 °C with a resolution of ∼2 cm^{-1} with 600 g/mm grating and ∼1 cm^{-1} with 1200 g/mm grating. The setup is carefully calibrated by using mercury lamp and cyclohexane (mode at 801.3 cm^{-1}) before the Raman measurements.

3. RESULTS AND DISCUSSION

In previous reports, it has been suggested that the intrinsic intermittency and inhomogeneity of the single molecule interfacial ET dynamics are directly related to electronic coupling at the molecule−semiconductor interface.[1−4] To obtain further insight into the electric field effect on the coupling properties at the interface, the alizarin−TiO_2 system has been chosen (Figure 1C,D) since it is a typical system with strong interfacial electronic coupling.

Figure 2 displays the characteristic SERS spectra of alizarin−TiO_2 system with the typical free alizarin vibrations and an additional peak at 648 cm^{-1} corresponding to Ti−O stretching mode from bridging Ti−O−C.[11a,53,57,58] The strong C−O stretching mode at 1330 cm^{-1} suggests that binding of hydroxyl groups of alizarin to a Ti of TiO_2 surface generates the alizarin−TiO_2 interfacial charge transfer complex. In the absence of the external potential, both the bridging mode and free alizarin vibrations do not display vibrational shifts (Figure S1 shows

DOI: 10.1021/jacs.5b10253
J. Am. Chem. Soc. 2016, 138, 1536−1542

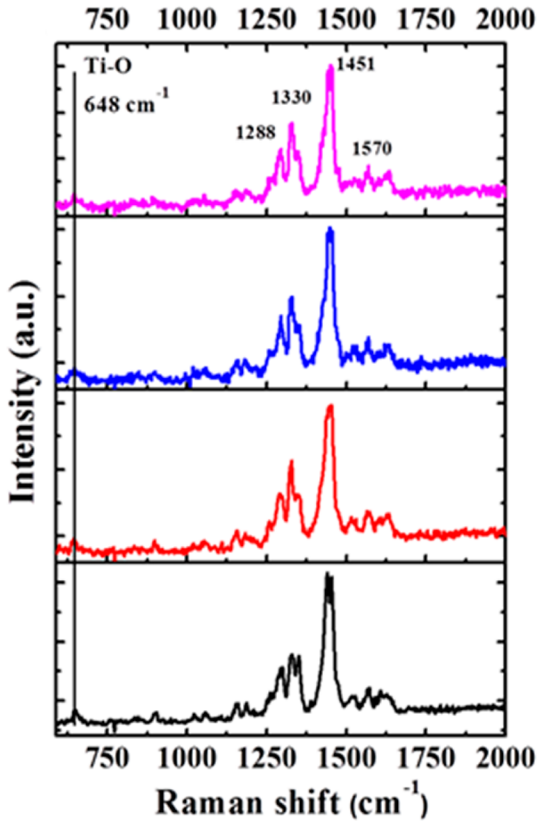

Figure 2. Four consecutive SMSERS spectra (20 s/spectrum) showing the typical Ti−O stretching mode from bridging Ti−O−C which suggests the strong electronic coupling at the interface. All the spectra were collected from different hot spots.

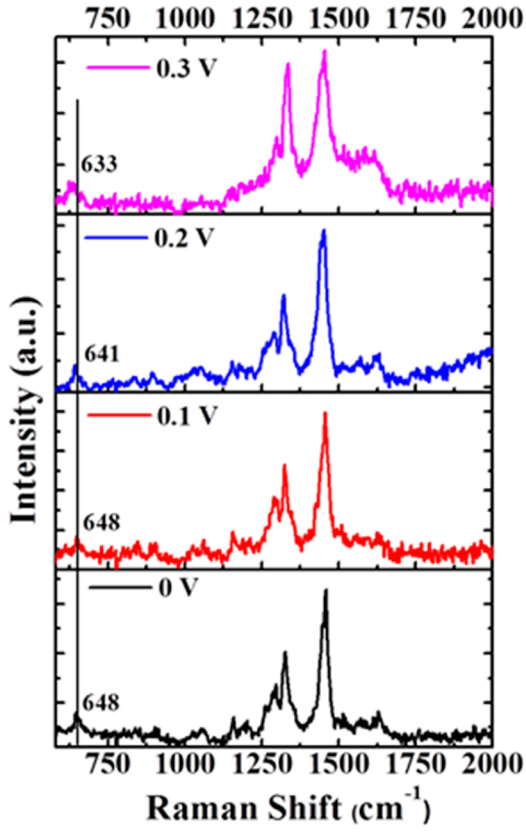

Figure 3. SMSERS spectra of alizarin−TiO_2 complex from same hot spot under 0, 0.1, 0.2, and 0.3 V, respectively.

distribution of 648 cm^{-1} peak obtained from different hot spots in the absence of external potential. Figure S2 shows Raman spectrum of TiO_2 without alizarin). Typically, the Raman spectra exhibit blinking and single step photobleaching, which suggests presence of a single or a small number of alizarin molecules at a hot spot.

EFE on the bridging vibrational mode of alizarin−TiO_2 interface is shown in Figure 3; while the characteristic free alizarin vibrations are stable in our experimental resolution (±2 cm^{-1}), as a result of the additional anharmonicity created within the interface bond via externally applied electric field, a prominent directional shift of the bridging mode from 648 to 641 and 633 cm^{-1} was observed under 0.2 and 0.3 V, respectively. However, the peak remains at its original position (648 cm^{-1}) for more than 95% of probed hot spots under 0.1 V (Figure S3). At higher applied potentials (0.2 V and 0.3 V), the shifts in Raman frequency were observed for majority of the probed hot spots; however, the Raman spectra from several hot spots were still found to retain the original peak at 648 cm^{-1}. The difference of each hot spot behavior and the distribution of Raman shifts are attributed to the interactions changes and fluctuations at the Alizarin−TiO_2 interface associated with inhomogeneity on the surface in each hot spot. Nevertheless, the pronounced frequency shift in relation to increase in the field strength is consistent with the theory; first, the displacement created in the average position of the lowest and the first vibrational levels is directly related with the applied potential; and second, harmonic force constant varies due to the electronic polarizability and results in weakening of the interface bond.[27,31,36]

In addition to the anharmonicity-driven vibrational shift, the interfacial Ti−O Raman band shows strong fluctuations especially under the external potential (Figure S3). It has been reported that the single-molecule SERS fluctuation originates from interaction changes and fluctuations at the molecule−substrate interface,[61−69] thermal effect,[16,70,71] and isotopic effect.[66] Isotopic effect is a rare and unique event unlikely to occur in our system. The fluctuations and changes in interfacial interactions arise from fluctuation of the surface work functions of the substrates, nanoscale inhomogeneous field distribution of the excitation light, structural differences of metallic surfaces, molecular motions, and electron transfer occurrences. Additionally, the nanoscale inhomogeneities, the electric field distribution on the layer depending on the distance from the source, and the heterogeneity of the electric field may result in inhomogeneous field felt by the adsorbed molecule on TiO_2 NP surface, consequently the magnitude of fluctuations varies from hot spot to hot spot. Furthermore, we should point out that in our system there is an additional cause more likely to give rise to the interaction changes and fluctuations. It has been reported previously that the peak position and the shape of the surface plasmon band of the silver NP exhibit prominent changes under the applied potential at the electrode surface, and also, the absorbance of the particles has been observed to display time dependence.[72] The perturbation of the surface-plasmon polaritons of Ag NP may give rise to the change in the surface work function and alteration of the interaction with the molecule. Another phenomenon occurs by virtue of the perturbation created is that the energy of the surface-plasmon

DOI: 10.1021/jacs.5b10253
J. Am. Chem. Soc. 2016, 138, 1536−1542

polaritons shifts to a different energy level, causing the loss of the surface-enhancement due to being less resonant with the excitation wavelength,[35] which is more likely responsible for the low SERS intensity during our measurements.

During our measurements, additional to the shift of the peak position, occurrence of splitting in 631 ± 2 cm^{-1} and 661 ± 2 cm^{-1}, instead of 648 cm^{-1} has also been observed, for example, under 0.3 V (Figure 4). However, the occurrence of splitting is

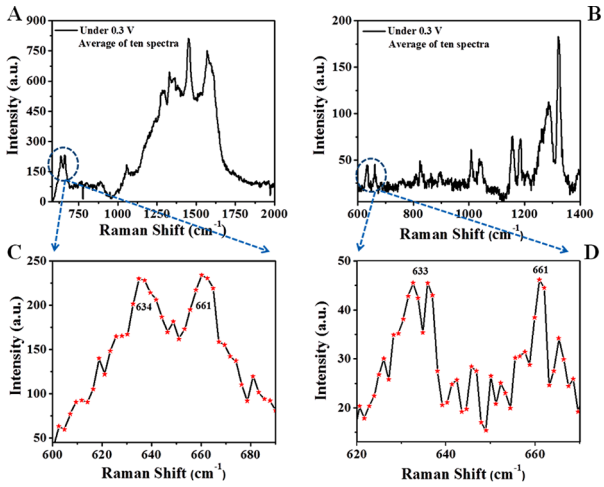

Figure 4. (A) and (B) are average of ten SMSERS spectra (20 s/spectrum) of alizarin−TiO_2 complex under 0.3 V potential with 600 g/mm and 1200 g/mm grating, respectively. All the spectra with a specific grating were collected from same hot spots. (C) and (D) are the zoomed-in view of the splitting for the spectra in A and B.

low, and it has been observed for about less than 10−20% of the probed hot spots. To obtain higher resolution and ensure the occurrence of splitting, measurements were also performed with a higher resolution of ±1 cm^{-1} by using a 1200 g/mm monochromator grating (Figure 4B and 4D). We suggest that the splitting is due to a few reasons: (1) It is likely that the peak position fluctuates in between two states under our experimental time resolution (20 s/spectrum), the resultant spectrum is the averaged out spectra of the two states. (2) The splitting may also be due to the Fermi resonance,[44] defined as the mixing of two vibrational levels which lies energetically close to each other.[44,73] This phenomenon, first observed by Fermi in CO_2, is caused by anharmonicity of the system and is known as a classical example of vibrational anharmonicity.[44,74,75] This effect has been observed by infrared spectroscopy both in the presence[42] and the absence[76] of the external potential and previously by Raman spectroscopy[77] in the absence of the potential. In our system, the applied external electric field results in an additional vibrational anharmonicity in the system which can result in the Fermi resonance. (3) Considering bonding occurred via both hydroxyl groups, it is also possible that while one of the interface bonds is getting stronger the other one is getting weaker under the potential causing the occurrence of two separate peaks. Similar observation has been reported previously. For example, Liu et al. reported voltage-dependent peak splitting of ∼22 cm^{-1} and suggested that it is due to the different coupling strength between the gold tip and gold substrate to 4,4′-bipyridine molecule under applied potential.[10] (4) Another plausible reason may be Stark effect induced by applied electric field, observed in many studies.[49,78−82] However, we have observed similar shifting and splitting in case of applied positive and negative electric fields (vide infra), which is unlike Stark effect. The Stark effect should have directional frequency shift depending on applied positive and negative electric fields, although the orientation of the local electric field may be complex due to the inhomogeneous interfacial topography. Nevertheless, on the basis of these observations, we attribute that the Stark effect is not a dominant factor for our system.

In addition to the positive potentials, we have also performed the experiments under negative potentials. As positive potentials, the same magnitude and direction of the shift/splitting with the corresponding potential strength were observed with applied negative potential (Figure 5). As the

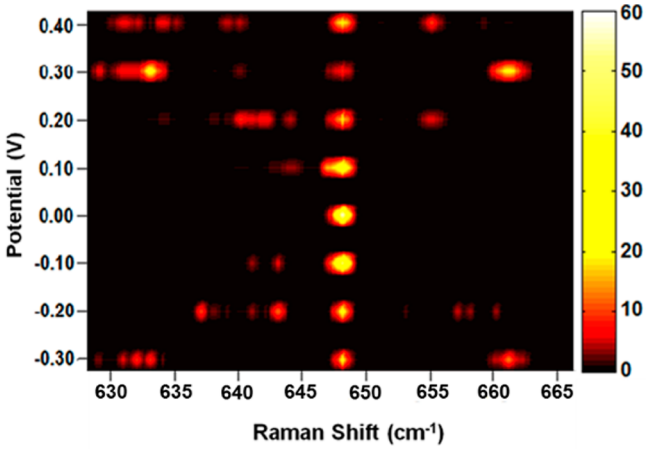

Figure 5. 2-D distribution of the Ti−O bridging peak positions under both positive and negative potentials (0.4, 0.3, 0.2, 0.1, 0.0, −0.1, −0.2, and −0.3 V). For each applied potential 60 spectra from different hot spots, i.e., a total of 480 spectra, were used to build this 2-D distribution.

applied electric potential increases from 0.3 to 0.4 V, the changes of the interfacial Ti−O bridging mode energy are increasingly more inhomogeneous and complex (Figure 5), which is most likely associated with the complex interfacial topography, inhomogeneous electric field of the applied potential at the interface, molecular ground state electrochemical responses,[72,82d] and the gradient near-field of the laser illumination.[11b,83] Nevertheless, further research is definitely warranted in order to reach a complete comprehension of the physical origins of the Raman spectral responses we reported here.

To further analyze the origin of the peak splitting in the presence of electric field, we performed density functional theory (DFT) calculations. Our model considers that the attachment of alizarin to TiO_2 occurs through two hydroxyl oxygen bonded with single or two separate Ti atoms. Alizarin is attached to Ti (IV) centers of $(TiO_2)_{15}$ bulk, which is frozen in the configuration, in bidentate mode and optimized by using B3PW91 functional, with the LANL2DZ basis set on Ti atoms, and a 6-31G(d) basis set on all other atoms. It should be noted that this simplified model of alizarin−TiO_2 complex does not intend to simulate the actual surface of TiO_2, but only to provide a basis for the discussion of the experimental evidence obtained in the Raman spectrum of the proposed interfacial Ti−O binding modes. Raman spectra of the complex are calculated by applying the multipole electric field in the direction normal to the TiO_2 surface with no symmetry. The

DOI: 10.1021/jacs.5b10253
J. Am. Chem. Soc. 2016, 138, 1536−1542

spectra are plotted without using any scaling factor. All DFT calculations have been performed with Gaussian 09 package.[84]

The charge distribution in the absence and the presence of the electric field is shown in Figure 6A and Figure 6B,

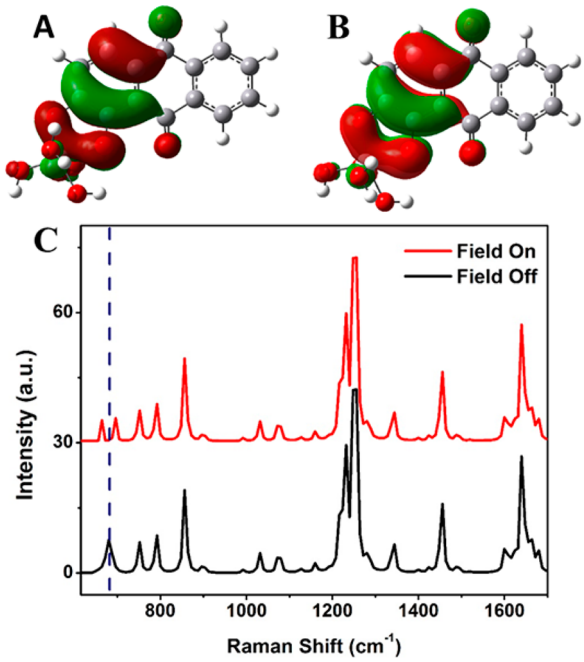

Figure 6. DFT calculations of alizarin−TiO_2 system. Charge distribution in the (A) absence and (B) presence of static multipole electric field of 5.0×10^5 V m^{-1} in the direction perpendicular to the TiO_2 substrate and (C) calculated Raman spectra of corresponding structures. Presence of two prominent peaks in the presence of electric field is the clear indication of the effect of electric field on interfacial Ti−O bonds.

respectively. The substantial change of the charge distribution especially in the proximity of the Ti−O−C bonding suggests the sensitivity of the interface bonding to electric field. The calculations showed small change in bond length for both interface bonds: elongation of the interface bond in proximity to carbonyl group ∼0.09 Å and the shortening of the second interface bond ∼0.04 Å, and the corresponding calculated Raman spectra displays two peaks with ∼32 cm^{-1} peak-to-peak distance (Figure 6c) (see Figures S4 and S5 for splitting of peak under positive and negative electric field, respectively). Additionally, for the free alizarin vibrations, maximum 4 cm^{-1} shift of the peak positions toward the lower energy and intensity changes has been observed.

The attachment of alizarin molecule with two hydroxyl oxygens linked to a surface Ti atom makes the configuration slightly tilted[78a] to the nanoparticle surface resulting in two unsymmetrical Ti−O bonds. Two Ti−O surface bonds resonate at different vibrational frequency under an applied electric field due to redistribution of charge density across the alizarin−TiO_2 interface as shown in Figure 7. The distribution of the local interfacial electric field coupled with bonding electrons creates stabilized and destabilized interactions to the surface Ti−O bonds, slightly changing the bond force constants asymmetrically. Since Raman spectroscopy is sensitive to the bond orientation and strength, local electric field created at the interface can be considered as the major source of the asymmetric interfacial covalent bond vibration. Even though,

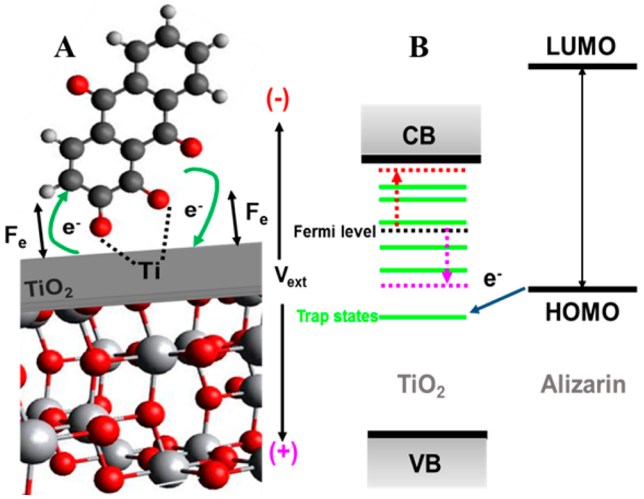

Figure 7. Schematic illustration of (A) alizarin adsorbed on TiO_2 surface and interfacial electric field and (B) energy states and electronic delocalization at the alizarin−TiO_2 interface. Applied negative and positive potential shift the TiO_2 Fermi level up (red) and down (pink), respectively. F_e, electric field; V_{ext}, applied potential; VB, valence band; CB, conduction band.

the DFT calculations show correlation with the experimental data and suggests that there occurs a field-induced electronic coupling change, more investigation is necessary to fully understand all the contributing factors.

In light of the data presented, we suggest that the vibrational energy levels and as a result the electronic coupling of the molecule−semiconductor complex, undergo significant field-induced changes. Previously, it has been established that interfacial ET dynamics is directly related with the electronic coupling as well as the vibrational relaxation energy of the adsorbed molecules and surface vibrational modes of the semiconductor.[11a,57] According to nonadiabatic ET theory, the rate of electron transfer, k_{ET} can be expressed as the sum of ET rates to all possible accepting states in the semiconductor.[1]

$$k_{ET} = \frac{2\pi}{\hbar}\int_{-\infty}^{\infty} dE\rho(E)(1 - f(E, E_F))|H(E)|^2 \times \frac{1}{\sqrt{4\pi\lambda k_B T}}\exp\left[-\frac{(\lambda + \Delta G_0 + E)^2}{4\lambda k_B T}\right] \quad (1)$$

ΔG_0 is driving force for electron injection; $\rho(E)$ is the density of states (DOS) at energy E relative to the conduction band edge, which can include both bulk states and surface states; $H(E)$ is the average electronic coupling between the adsorbate excited state and all states in the semiconductor at the same energy E; $f(E, E_F)$ is the Fermi occupancy factor; and λ is the total reorganization energy. A particular vibrational mode change can effectively change ET rate by changing ΔG_0, DOS, electronic coupling and most importantly by changing λ value. The total reorganization energy, λ is contribution of both vibrational reorganization energy, λ_V and solvent reorganization energy, λ_S. Under consideration of harmonic vibrations λ_V can be represented as[11a,82a]

$$\lambda_V = 0.5\sum \Delta_k{}^2 \nu_k \quad (2)$$

Where ν is vibrational frequency for a particular mode, and Δ is displacement in dimensionless normal coordinates between ground- and excited-state equilibrium geometries along each

DOI: 10.1021/jacs.5b10253
J. Am. Chem. Soc. 2016, 138, 1536−1542

normal coordinate. Although our results suggest electric field dependence of ET rate, the quantitative information about ET rate change with change in particular vibrational mode frequency requires further research.

Nevertheless, electronic delocalization and redistribution at the perturbed alizarin−TiO_2 interface under the electric field (Figure 7B) have significant impact on the interfacial covalent bonds. Therefore, the field-induced shift or splitting are expected to have a prominent influence on the interfacial ET rates due to the driving force as well as electronic coupling changes.[78b] The dynamics of ET from alizarin to TiO_2 are modulated by the fluctuations of interfacial bond vibrational energy induced by the static electric field developed at the interface which in turn changes the electronic coupling leading to ET intermittency.[85−87] Generally, the interfacial electric potential can be applied externally,[88] as this work shows, or generated intrinsically due to the excess charge accumulation at the molecule−TiO_2 interfaces, as shown in many dye-sensitized TiO_2 solar energy conversion systems.[34,35,48−50] The excess charge accumulation, diffusion, and dissipation are stochastic, and in turn, the interfacial electric potential originated from the excess charges presumably involves significant fluctuations at spatially inhomogeneous interacting sites of nanoparticle, which likely impact the interfacial electron transfer rate processes. Therefore, the coupling energy changes may serve as a prominent and intrinsic origin of the complex interfacial electron transfer dynamics, such as the intermittent interfacial electron transfer dynamics observed by single-molecule photon-stamping spectroscopy measurements.[4,85−87]

4. CONCLUSION

The electric field effect on the interface properties has been probed by using single-hot spot microscopic surface-enhanced Raman spectroscopy and supported by density functional theory calculations in alizarin−TiO_2 system. The perturbation, created by the external potential, has been observed to cause a shift and/or splitting of the 648 cm^{-1} peak, typical indicator of the coupling energy changes between alizarin and TiO_2. Such splitting provides evidence for electric field-dependent electronic coupling changes that have a significant impact on the interfacial electron transfer dynamics, especially on the temporal and spatial inhomogeneity and fluctuation of the interfacial electron transfer rate processes. The electric field effect, due to the external electric field application or the inhomogeneous static charge accumulation at the interface of dye−TiO_2 nanoparticles, suggests that the interfacial electron transfer dynamics is intrinsically inhomogeneous with static and dynamic disorders, showing the reactivity intermittency[4,85−87] at the individual molecule level. A detailed understanding of the related interface properties and the factors affecting the molecule−semiconductor interactions is crucial for fundamental interfacial and surface chemistry and physics, as well as for further development and commercialization of the applications such as photovoltaic devices and molecular devices.

■ ASSOCIATED CONTENT

Supporting Information

The Supporting Information is available free of charge on the ACS Publications website at DOI: 10.1021/jacs.5b10253.

2-D distribution of bridging mode Raman shift without and with applied potential, Raman spectrum without alizarin, and calculated Raman spectra at applied electric fields. (PDF)

■ AUTHOR INFORMATION

Corresponding Author

*hplu@bgsu.edu

Author Contributions

†V.G.R. and Y.W. contributed equally.

Notes

The authors declare no competing financial interest.

■ ACKNOWLEDGMENTS

This work was supported by the US Department of Energy (DOE), Office of Basic Energy Sciences, Division of Chemical Sciences, Geosciences & Biosciences. We thank Prof. Alexey T. Zayak for stimulating discussions. Our DFT calculation was carried out by using the computer facility of the Ohio Supercomputer Center (OSC), Columbus, Ohio.

■ REFERENCES

(1) Anderson, N. A.; Lian, T. Q. *Annu. Rev. Phys. Chem.* **2005**, *56*, 491.
(2) Watson, D. F.; Meyer, G. J. *Annu. Rev. Phys. Chem.* **2005**, *56*, 119.
(3) Duncan, W. R.; Prezhdo, O. V. *Annu. Rev. Phys. Chem.* **2007**, *58*, 143.
(4) Wang, Y.; Wang, X.; Ghosh, S. K.; Lu, H. P. *J. Am. Chem. Soc.* **2009**, *131*, 1479.
(5) Hochstrasser, R. M. *Acc. Chem. Res.* **1973**, *6*, 263.
(6) Chattopadhyay, A.; Boxer, S. G. *J. Am. Chem. Soc.* **1995**, *117*, 1449.
(7) Bagus, P. S.; Nelin, C. J.; Müller, W.; Philpott, M. R.; Seki, H. *Phys. Rev. Lett.* **1987**, *58*, 559.
(8) Suydam, I. T.; Boxer, S. G. *Biochemistry* **2003**, *42*, 12050.
(9) Lakshmi, S.; Dutta, S.; Pati, S. K. *J. Phys. Chem. C* **2008**, *112*, 14718.
(10) Liu, Z.; Ding, S.-Y.; Chen, Z.-B.; Wang, X.; Tian, J.-H.; Anema, J. R.; Zhou, X.-S.; Wu, D. Y.; Mao, B.-W.; Xu, X.; Ren, B.; Tian, Z.-Q. *Nat. Commun.* **2011**, *2*, 305.
(11) (a) Pan, D.; Hu, D.; Lu, H. P. *J. Phys. Chem. B* **2005**, *109*, 16390. (b) Pan, D.; Klymyshyn, N.; Hu, D.; Lu, H. P. *Appl. Phys. Lett.* **2006**, *88*, 093121.
(12) Kneipp, K.; Wang, Y.; Kneipp, H.; Perelman, L. T.; Itzkan, I.; Dasari, R. R.; Feld, M. S. *Phys. Rev. Lett.* **1997**, *78*, 1667.
(13) Nie, S.; Emery, S. R. *Science* **1997**, *275*, 1102.
(14) Michaels, A. M.; Nirmal, M.; Brus, L. E. *J. Am. Chem. Soc.* **1999**, *121*, 9932.
(15) Weiss, A.; Haran, G. *J. Phys. Chem. B* **2001**, *105*, 12348.
(16) Wang, Z. J.; Rothberg, L. J. *J. Phys. Chem. B* **2005**, *109*, 3387.
(17) (a) Dieringer, J. A.; Wustholz, K. L.; Masiello, D. J.; Camden, J. P.; Kleinman, S. L.; Schatz, G. C.; Van Duyne, R. P. *J. Am. Chem. Soc.* **2009**, *131*, 849. (b) Camden, J. P.; Dieringer, J. A.; Wang, Y.; Masiello, D. J.; Marks, L. D.; Schatz, G. C.; Van Duyne, R. P. *J. Am. Chem. Soc.* **2008**, *130*, 12616. (c) Stiles, P.; Dieringer, J.; Shah, N. C.; Van Duyne, R. P. *Annu. Rev. Anal. Chem.* **2008**, *1*, 601.
(18) Hush, N. S.; Williams, M. L. *J. Mol. Spectrosc.* **1974**, *50*, 349.
(19) Gready, J. E.; Bacskay, G. B.; Hush, N. S. *Chem. Phys.* **1978**, *31*, 467.
(20) Lambert, D. K. *Solid State Commun.* **1984**, *51*, 297.
(21) Lambert, D. K. *J. Chem. Phys.* **1988**, *89*, 3847.
(22) Hush, N. S.; Reimers, J. R. *J. Phys. Chem.* **1995**, *99*, 15798.
(23) Reimers, J. R.; Zeng, J.; Hush, N. S. *J. Phys. Chem.* **1996**, *100*, 1498.
(24) Reimers, J. R.; Hush, N. S. *J. Phys. Chem. A* **1999**, *103*, 10580.
(25) Treynor, T. P.; Boxer, S. G. *J. Phys. Chem. A* **2004**, *108*, 1764.
(26) Brewer, S. H.; Franzen, S. *J. Chem. Phys.* **2003**, *119*, 851.
(27) Bishop, D. M. *J. Chem. Phys.* **1993**, *98*, 3179.

DOI: 10.1021/jacs.5b10253
J. Am. Chem. Soc. 2016, 138, 1536−1542

(28) Pierce, D. W.; Boxer, S. G. *Biophys. J.* **1995**, *68*, 1583.
(29) Bublitz, G. U.; Boxer, S. G. *Annu. Rev. Phys. Chem.* **1997**, *48*, 213.
(30) Andrews, S. S.; Boxer, S. G. *J. Phys. Chem. A* **2000**, *104*, 11853.
(31) Andrews, S. S.; Boxer, S. G. *J. Phys. Chem. A* **2002**, *106*, 469.
(32) Kriegl, J. M.; Nienhaus, K.; Deng, P. C.; Fuchs, J.; Nienhaus, G. U. *Proc. Natl. Acad. Sci. U. S. A.* **2003**, *100*, 7069.
(33) Park, E. S.; Boxer, S. G. *J. Phys. Chem. B* **2002**, *106*, 8910.
(34) Oklejas, V.; Sjostrom, C.; Harris, J. M. *J. Am. Chem. Soc.* **2002**, *124*, 2408.
(35) Oklejas, V.; Sjostrom, C.; Harris, J. M. *J. Phys. Chem. B* **2003**, *107*, 7788.
(36) (a) Park, E. S.; Boxer, S. G. *J. Phys. Chem. B* **2002**, *106*, 5800. (b) Li, Y.; Doak, P.; Kronik, L.; Neaton, J. B.; Natelson, D. *Proc. Natl. Acad. Sci. U. S. A.* **2014**, *111*, 1282.
(37) Levinson, N. M.; Bolte, E. E.; Miller, C. S.; Corcelli, S. A.; Boxer, S. G. *J. Am. Chem. Soc.* **2011**, *133*, 13236.
(38) Xu, L.; Cohen, A. E.; Boxer, S. G. *Biochemistry* **2011**, *50*, 8311.
(39) Webb, L. J.; Boxer, S. G. *Biochemistry* **2008**, *47*, 1588.
(40) Park, E. S.; Andrews, S. S.; Hu, R. B.; Boxer, S. G. *J. Phys. Chem. B* **1999**, *103*, 9813.
(41) Treynor, T. P.; Boxer, S. G. *J. Phys. Chem. B* **2004**, *108*, 13513.
(42) Park, E. S.; Thomas, M. R.; Boxer, S. G. *J. Am. Chem. Soc.* **2000**, *122*, 12297.
(43) Badger, R. M. *J. Chem. Phys.* **1934**, *2*, 128.
(44) Fermi, E. Z. *Eur. Phys. J. A* **1931**, *71*, 250.
(45) Suydam, I. T.; Snow, C. D.; Pande, V. S.; Boxer, S. G. *Science* **2006**, *313*, 200.
(46) Lehle, H.; Kriegl, J. M.; Nienhaus, K.; Deng, P. C.; Fengler, S.; Nienhaus, G. U. *Biophys. J.* **2005**, *88*, 1978.
(47) Treynor, T. P.; Yoshina-Ishii, C.; Boxer, S. G. *J. Phys. Chem. B* **2004**, *108*, 13523.
(48) Staniszewski, A.; Ardo, S.; Sun, Y.; Castellano, F. N.; Meyer, G. J. *J. Am. Chem. Soc.* **2008**, *130*, 11586.
(49) (a) Ardo, S.; Sun, Y.; Staniszewski, A.; Castellano, F. N.; Meyer, G. J. *J. Am. Chem. Soc.* **2010**, *132*, 6696. (b) O'Donnell, R. M.; Sampaio, R. N.; Barr, T. J.; Meyer, G. J. *J. Phys. Chem. C* **2014**, *118*, 16976.
(50) Johansson, P. G.; Kopecky, A.; Galoppini, E.; Meyer, G. J. *J. Am. Chem. Soc.* **2013**, *135*, 8331.
(51) Persson, P.; Bergstrom, R.; Lunell, S. *J. Phys. Chem. B* **2000**, *104*, 10348.
(52) Rajh, T.; Chen, L. X.; Lukas, K.; Liu, T.; Thurnauer, M. C.; Tiede, D. M. *J. Phys. Chem. B* **2002**, *106*, 10543.
(53) Shoute, L. C. T.; Loppnow, G. R. *J. Chem. Phys.* **2002**, *117*, 842.
(54) Duncan, W. R.; Prezhdo, O. V. *J. Phys. Chem. B* **2005**, *109*, 365.
(55) Duncan, W. R.; Stier, W. M.; Prezhdo, O. V. *J. Am. Chem. Soc.* **2005**, *127*, 7941.
(56) Kondov, I.; Wang, H. B.; Thoss, M. *Int. J. Quantum Chem.* **2006**, *106*, 1291.
(57) Sevinc, P. C.; Wang, X.; Wang, Y.; Zhang, D.; Meixner, A. J.; Lu, H. P. *Nano Lett.* **2011**, *11*, 1490.
(58) Sekiya, T.; Ohta, S.; Kamei, S.; Hanakawa, M.; Kurita, S. *J. Phys. Chem. Solids* **2001**, *62*, 717.
(59) Leopold, N.; Lendl, B. *J. Phys. Chem. B* **2003**, *107*, 5723.
(60) Duonghong, D.; Borgarello, E.; Gratzel, M. *J. Am. Chem. Soc.* **1981**, *103*, 4685.
(61) Bosnick, K. A.; Jiang, J.; Brus, L. E. *J. Phys. Chem. B* **2002**, *106*, 8096.
(62) Lukatsky, D. B.; Haran, G.; Safran, S. A. *Phys. Rev. E: Stat. Phys., Plasmas, Fluids, Relat. Interdiscip. Top.* **2003**, *67*, 062402.
(63) Suh, Y. D.; Schenter, G. K.; Zhu, L. Y.; Lu, H. P. *Ultramicroscopy* **2003**, *97*, 89.
(64) Haran, G. *Isr. J. Chem.* **2004**, *44*, 385.
(65) Lu, H. P. *J. Phys.: Condens. Matter* **2005**, *17*, R333.
(66) Etchegoin, P. G.; Le Ru, E. C. *Anal. Chem.* **2010**, *82*, 2888.
(67) Wustholz, K. L.; Henry, A. I.; McMahon, J. M.; Freeman, R. G.; Valley, N.; Piotti, M. E.; Natan, M. J.; Schatz, G. C.; Van Duyne, R. P. *J. Am. Chem. Soc.* **2010**, *132*, 10903.
(68) Kim, H.; Kosuda, K. M.; Van Duyne, R. P.; Stair, P. C. *Chem. Soc. Rev.* **2010**, *39*, 4820.
(69) Bizzarri, A. R.; Cannistraro, S. *Phys. Rev. Lett.* **2005**, *94*, 068313−1.
(70) Stracke, F.; Blum, C.; Becker, S.; Mullen, K.; Meixner, A. J. *Chem. Phys. Lett.* **2000**, *325*, 196.
(71) Luo, Z. X.; Luo, Y.; Li, J.; Liu, K.; Fu, H. B.; Ma, Y.; Yao, J. N. *Chem. Commun.* **2009**, 1342.
(72) Ung, T.; Giersig, M.; Dunstan, D.; Mulvaney, P. *Langmuir* **1997**, *13*, 1773.
(73) Fujita, K.; Kimura, M. *Mol. Phys.* **1980**, *41*, 1203.
(74) Rodriguez-Garcia, V.; Hirata, S.; Yagi, K.; Hirao, K.; Taketsugu, T.; Schweigert, I.; Tasumi, M. *J. Chem. Phys.* **2007**, *126*, 124303.
(75) Burke, K.; Langreth, D. C.; Persson, M.; Zhang, Z. Y. *Phys. Rev. B: Condens. Matter Mater. Phys.* **1993**, *47*, 15869.
(76) Mcgee, K. C.; Capitano, A. T.; Grassian, V. H. *Langmuir* **1994**, *10*, 632.
(77) Nam, S. I.; Min, E. S.; Jung, Y. M.; Lee, M. S. *Bull Korean Chem. Soc.* **2001**, *22*, 989.
(78) (a) Nawrocka, A.; Krawczyk, S. *J. Phys. Chem. C* **2008**, *112*, 10233. (b) Monti, O. L. A. *J. Phys. Chem. Lett.* **2012**, *3*, 2342.
(79) Cappel, U. B.; Feldt, S. M.; Schöneboom, J.; Hagfeldt, A.; Boschloo, G. *J. Am. Chem. Soc.* **2010**, *132*, 9096.
(80) (a) Fried, S. D.; Boxer, S. G. *Acc. Chem. Res.* **2015**, *48*, 998. (b) Boxer, S. G. *J. Phys. Chem. B* **2009**, *113*, 2972.
(81) Finkelstein, I. J.; Goj, A.; McClain, B. L.; Massari, A. M.; Merchant, K.; Loring, R. F.; Fayer, M. D. *J. Phys. Chem. B* **2005**, *109*, 16959.
(82) (a) Hupp, J. T.; Williams, R. D. *Acc. Chem. Res.* **2001**, *34*, 808. (b) Yoon, D. I.; Selmarten, D. C.; Lu, H.; Liu, H.; Mottley, C.; Ratner, M. A.; Hupp, J. T. *Chem. Phys. Lett.* **1996**, *251*, 84. (c) Karki, L.; Lu, H. P.; Hupp, J. T. *J. Phys. Chem.* **1996**, *100*, 15637. (d) Lemon, B. I.; Hupp, J. T. *J. Phys. Chem. B* **1999**, *103*, 3797.
(83) (a) Ayars, E. J.; Hallen, H. D.; Jahncke, C. L. *Phys. Rev. Lett.* **2000**, *85*, 4180. (b) Schlücker, S. *Angew. Chem., Int. Ed.* **2014**, *53*, 4756. (c) Bailo, E.; Deckert, V. *Chem. Soc. Rev.* **2008**, *37*, 921.
(84) Frisch, M. J.; Trucks, G. W.; Schlegel, H. B.; Scuseria, G. E.; Robb, M. A.; Cheeseman, J. R.; Scalmani, G.; Barone, V.; Mennucci, B.; Petersson, G. A.; Nakatsuji, H.; Caricato, M.; Li, X.; Hratchian, H. P.; Izmaylov, A. F.; Bloino, J.; Zheng, G.; Sonnenberg, J. L.; Hada, M.; Ehara, M.; Toyota, K.; Fukuda, R.; Hasegawa, J.; Ishida, M.; Nakajima, T.; Honda, Y.; Kitao, O.; Nakai, H.; Vreven, T.; Montgomery, J. A., Jr.; Peralta, J. E.; Ogliaro, F.; Bearpark, M.; Heyd, J. J.; Brothers, E.; Kudin, K. N.; Staroverov, V. N.; Kobayashi, R.; Normand, J.; Raghavachari, K.; Rendell, A.; Burant, J. C.; Iyengar, S. S.; Tomasi, J.; Cossi, M.; Rega, N.; Millam, J. M.; Klene, M.; Knox, J. E.; Cross, J. B.; Bakken, V.; Adamo, C.; Jaramillo, J.; Gomperts, R.; Stratmann, R. E.; Yazyev, O.; Austin, A. J.; Cammi, R.; Pomelli, C.; Ochterski, J. W.; Martin, R. L.; Morokuma, K.; Zakrzewski, V. G.; Voth, G. A.; Salvador, P.; Dannenberg, J. J.; Dapprich, S.; Daniels, A. D.; Farkas, Ö.; Foresman, J. B.; Ortiz, J. V.; Cioslowski, J.; Fox, D. J. *Gaussian 09*, revision C.01; Gaussian, Inc.: Wallingford, CT, 2010.
(85) Guo, L.; Wang, Y.; Lu, H. P. *J. Am. Chem. Soc.* **2010**, *132*, 1999.
(86) Biju, V.; Micic, M.; Hu, D.; Lu, H. P. *J. Am. Chem. Soc.* **2004**, *126*, 9374.
(87) (a) Rao, V. G.; Dhital, B.; He, Y.; Lu, H. P. *J. Phys. Chem. C* **2014**, *118*, 20209. (b) Rao, V. G.; Dhital, B.; Lu, H. P. *J. Phys. Chem. B* **2015**, DOI: 10.1021/acs.jpcb.5b08807.
(88) Rao, V. G.; Dhital, B.; Lu, H. P. *Chem. Commun.* **2015**, *51*, 16821.

DOI: 10.1021/jacs.5b10253
J. Am. Chem. Soc. 2016, 138, 1536−1542